© 2017. Published by The Company of Biologists Ltd | Development (2017) 144, 4159-4172 doi:10.1242/dev.153288

RESEARCH ARTICLE

Graf regulates hematopoiesis through GEEC endocytosis of EGFR

Sungdae Kim[1,*], Minyeop Nahm[2,*], Najin Kim[1], Yumi Kwon[3], Joohyung Kim[4], Sukwoo Choi[5], Eun Young Choi[6], Jiwon Shim[7], Cheolju Lee[3] and Seungbok Lee[1,2,4,‡]

ABSTRACT

GTPase regulator associated with focal adhesion kinase 1 (GRAF1) is an essential component of the GPI-enriched endocytic compartment (GEEC) endocytosis pathway. Mutations in the human *GRAF1* gene are associated with acute myeloid leukemia, but its normal role in myeloid cell development remains unclear. We show that Graf, the *Drosophila* ortholog of GRAF1, is expressed and specifically localizes to GEEC endocytic membranes in macrophage-like plasmatocytes. We also find that loss of Graf impairs GEEC endocytosis, enhances EGFR signaling and induces a plasmatocyte overproliferation phenotype that requires the EGFR signaling cascade. Mechanistically, Graf-dependent GEEC endocytosis serves as a major route for EGFR internalization at high, but not low, doses of the predominant *Drosophila* EGFR ligand Spitz (Spi), and is indispensable for efficient EGFR degradation and signal attenuation. Finally, Graf interacts directly with EGFR in a receptor ubiquitylation-dependent manner, suggesting a mechanism by which Graf promotes GEEC endocytosis of EGFR at high Spi. Based on our findings, we propose a model in which Graf functions to downregulate EGFR signaling by facilitating Spi-induced receptor internalization through GEEC endocytosis, thereby restraining plasmatocyte proliferation.

KEY WORDS: Graf, GEEC endocytosis, EGFR, D-Cbl-mediated receptor ubiquitination, Plasmatocyte proliferation, *Drosophila*

INTRODUCTION

Epidermal growth factor receptor (EGFR) family members play pivotal roles in regulating cell proliferation and differentiation during animal development (Avraham and Yarden, 2011; Shilo, 2003). Their aberrant expression or activation is strongly associated with the etiology of several human epithelial cancers (Patel and Leung, 2012). Ligand binding to EGFR induces receptor dimerization and activation, which subsequently activates several downstream signaling cascades, including the Ras/mitogen-activated protein kinase (MAPK) and phosphatidylinositol 3-kinase (PI3K)/Akt pathways (Avraham and Yarden, 2011). In *Drosophila*, four ligands [i.e. Spitz (Spi), Karen, Gurken and Vein] activate a single EGFR to regulate many aspects of development, primarily via the canonical Ras-MAPK pathway (Shilo, 2003).

Ligand-induced activation of EGFR also triggers its rapid internalization to early endosomes, followed by either recycling to the plasma membrane or lysosomal degradation (Sorkin and Goh, 2009). Interestingly, two distinct modes of endocytosis differentially influence the fate of internalized EGFRs (Sigismund et al., 2008). Clathrin-dependent (CD) endocytosis, which functions at all EGF concentrations, leads to EGFR recycling and prolonged signaling. In contrast, clathrin-independent (CI) endocytosis, which is additionally activated under conditions of high EGF, is primarily linked to receptor degradation and signal attenuation. Although CI endocytosis of EGFR is known to be associated with Cbl-mediated receptor ubiquitylation at the plasma membrane (Sigismund et al., 2013), its precise molecular features remain poorly defined.

One prevalent type of CI endocytosis, which mediates the uptake of various GPI-anchored proteins (GPI-APs) as well as bulk fluid, involves the formation of pleiomorphic tubular intermediates known as clathrin-independent carriers (CLICs) (Kirkham et al., 2005; Sabharanjak et al., 2002). Once formed, CLICs undergo homotypic fusion to form glycosylphosphatidylinositol (GPI)-enriched endocytic compartments (GEECs), which then fuse with early/sorting endosomes derived from the CD endocytic system (Gupta et al., 2009; Kalia et al., 2006). This type of CI endocytosis has been shown to depend critically on the activity of the small GTPase Cdc42 and on GTPase regulator associated focal adhesion kinase 1 (GRAF1) (Lundmark et al., 2008; Sabharanjak et al., 2002).

GRAF1 contains N-terminal BIN/amphiphysin/Rvs (BAR) and pleckstrin homology (PH) domains that work together to generate and/or stabilize CLIC/GEEC endocytic membranes (Lundmark et al., 2008). In addition, this protein harbors a central RhoGAP domain that displays GAP activity toward Cdc42, raising the possibility that GRAF1 coordinates membrane remodeling and Cdc42-dependent actin polymerization to facilitate GEEC endocytosis. Apart from this role in endocytosis, GRAF1 has been implicated in regulation of myeloid cell development. Mutations and deletions in the human *GRAF1* gene are associated with acute myeloid leukemia (AML) or myelodysplastic syndrome (MDS) (Borkhardt et al., 2000). Furthermore, the *GRAF1* promoter is abnormally methylated in bone marrow samples from individuals with AML or MDS (Bojesen et al., 2006; Qian et al., 2011), reducing its expression (Qian et al., 2010). Despite these studies, it is unclear whether the two seemingly distinct roles of GRAF1 in hematopoiesis and GEEC endocytosis are related.

The *Drosophila* hematopoietic system provides a simple genetic model for the investigation of molecular aspects of myeloid cell development. *Drosophila* blood consists of only a few types of blood cells that functionally resemble the mammalian myeloid

[1]Interdisciplinary Graduate Program in Genetic Engineering, Seoul National University, Seoul 08826, Korea. [2]Department of Cell and Developmental Biology and Dental Research Institute, Seoul National University, Seoul 08826, Korea. [3]Center for Theragnosis, Korea Institute of Science and Technology, Seoul 02792, Korea. [4]Department of Brain and Cognitive Sciences, Seoul National University, Seoul 08826, Korea. [5]School of Biological Sciences, Seoul National University, Seoul 08826, Korea. [6]Department of Biomedical Sciences, Seoul National University, Seoul 08826, Korea. [7]Department of Life Science, Hanyang University, Seoul 04763, Korea.
*These authors contributed equally to this work

‡Author for correspondence (seunglee@snu.ac.kr)

S.L., 0000-0002-6620-6269

Received 10 April 2017; Accepted 2 October 2017

Development (2017) 144, 4159-4172 doi:10.1242/dev.153288

lineage. In addition, several key mechanisms controlling hematopoiesis are evolutionarily conserved (Crozatier and Vincent, 2011; Evans et al., 2003). Hematopoiesis in *Drosophila* occurs in two phases during development (Evans et al., 2003). The first phase takes place within the embryonic head mesoderm (Lebestky et al., 2000; Tepass et al., 1994) and produces two major classes of blood cells or hemocytes: macrophage-like plasmatocytes involved in phagocytosis and megakaryocyte-like crystal cells involved in melanization. The second phase of hematopoiesis occurs in larval lymph glands (LGs), which do not release differentiated plasmatocytes and crystal cells into circulation until the onset of pupariation (Holz et al., 2003). Lamellocytes, the final hemocyte type, are rarely found in normal healthy larvae but differentiate in response to parasitic infections (Lanot et al., 2001).

To understand the role of the GRAF protein family in blood cell development, we have studied the *Drosophila* GRAF1 ortholog Graf. Graf is expressed at high levels in plasmatocytes, where it plays an essential role in GEEC endocytosis. We provide evidence that Graf functions cell-autonomously to restrain plasmatocyte proliferation by inhibiting EGFR signaling. Consistent with this, EGFR signaling has been shown to stimulate plasmatocyte proliferation (Asha et al., 2003; Zettervall et al., 2004). Notably, GEEC endocytosis acts as a major pathway for EGFR internalization at high Spi and is preferentially associated with receptor degradation and signal attenuation. Finally, we find that high Spi treatment induces EGFR ubiquitylation mediated by *Drosophila* Cbl (D-Cbl), and that this modification subsequently promotes receptor association with Graf. This is the first demonstration of a role for Graf-dependent GEEC endocytosis in downregulating a specific signaling pathway and reveals a molecular mechanism underlying the recruitment of ubiquitylated cargoes to this CI endocytic pathway.

RESULTS

Isolation of a *Graf*-null mutant

A BLAST search using the human GRAF1 sequence identified a single *Drosophila* homolog: Graf (CG8948). Conversely, a search using *Drosophila* Graf showed the closest matches to three members of the human GRAF family of RhoGAPs (GRAF1-GRAF3). The *Drosophila* Graf protein has an identical domain organization (Fig. 1A) and overall 43-46% identity to its human homologs. The *Graf* gene spans ∼9.0 kb of genomic DNA and contains another gene (i.e. *CG8260*) within its second intron (Fig. 1B).

To generate *Graf*-null mutants, we imprecisely excised a P-element (G275) inserted in the *Graf* transcription unit (Fig. 1B). Sequence analysis identified a deletion ($Graf^{1}$) spanning the entire first exon and part of the first intron. Homozygous $Graf^{1}$ flies and heterozygotes over the deficiency *Df(1)BSC756* (hereafter referred to as *Df*) are null for *Graf* expression but express normal levels of the adjacent genes *mRpL3* and *CG8260* (Fig. 1C). Homozygous $Graf^{1}$ flies are viable and fertile.

Graf is expressed in the *Drosophila* hematopoietic system

To characterize the Graf protein, we raised an antibody against a Graf peptide (see Materials and Methods). In western blots of extracts derived from hemocytes of wild-type third instar larvae, this antibody detected a single major band of 110 kDa, the expected molecular weight of Graf, which was absent in extracts of $Graf^{1}/Df$ mutants (Fig. 2A). To prove this band corresponds to Graf, we transiently overexpressed the full-length protein in *Drosophila* S2R+ cells. Levels of the 110 kDa product were higher in extracts of transfected cells than in non-transfected cells (Fig. 2A).

To explore Graf expression in the embryonic hematopoietic system, we first analyzed wild-type and $Graf^{1}/Df$ embryos expressing a membrane-tethered GFP (*UAS-mCD8-GFP*) under the control of the hemocyte driver *srp-GAL4*. Double staining of wild-type embryos with anti-Graf and anti-GFP antibodies revealed Graf expression in the developing gut from stage 12 (data not shown), and beginning with stage 13, in migrating Srp-GFP^{+} plasmatocytes (Fig. 2B,C). Interestingly, Graf had a punctate distribution in embryonic plasmatocytes (Fig. 2B,C; enlargements). Although we observed some non-specific staining in the trachea and pharynx, we were unable to detect anti-Graf signal in the gut or Srp-GFP^{+} plasmatocytes of $Graf^{1}/Df$ embryos (Fig. 2D), confirming the specificity of anti-Graf staining. To examine Graf expression in

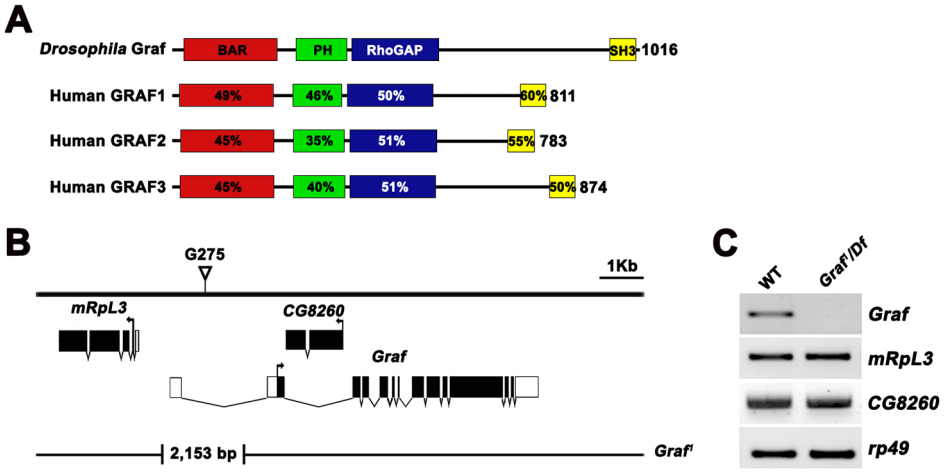

Fig. 1. Characterization of the *Drosophila Graf* gene and mutants. (A) Comparison of *Drosophila* Graf with human GRAF family proteins (GRAF1-GRAF3). Percentages indicate the sequence identity to *Drosophila* Graf in the BIN/amphiphysin/Rvs (BAR), pleckstrin homology (PH), RhoGAP and Src homology 3 (SH3) domains. (B) A genomic map of the *Graf* locus drawn based on annotated data from FlyBase (http://flybase.org/reports/FBgn0030685.html). Exon/intron organizations of *Graf* and its neighboring genes, *CG8260* and *mRpL3*, are shown. Untranslated regions are indicated by open boxes, translated regions by black boxes and translation initiation sites by arrows. The insertion site of P-element G275 is indicated by a triangle. Breakpoints of $Graf^{1}$ deletion generated via imprecise excision of G275 are indicated. (C) RT-PCR analysis of *Graf*, *CG8260* and *mRpL3* transcripts in wild-type (WT; w^{1118}) and $Graf^{1}/Df(1)BSC756$ ($Graf^{1}/Df$) third instar larvae. *rp49* is the loading control.

Development (2017) 144, 4159-4172 doi:10.1242/dev.153288

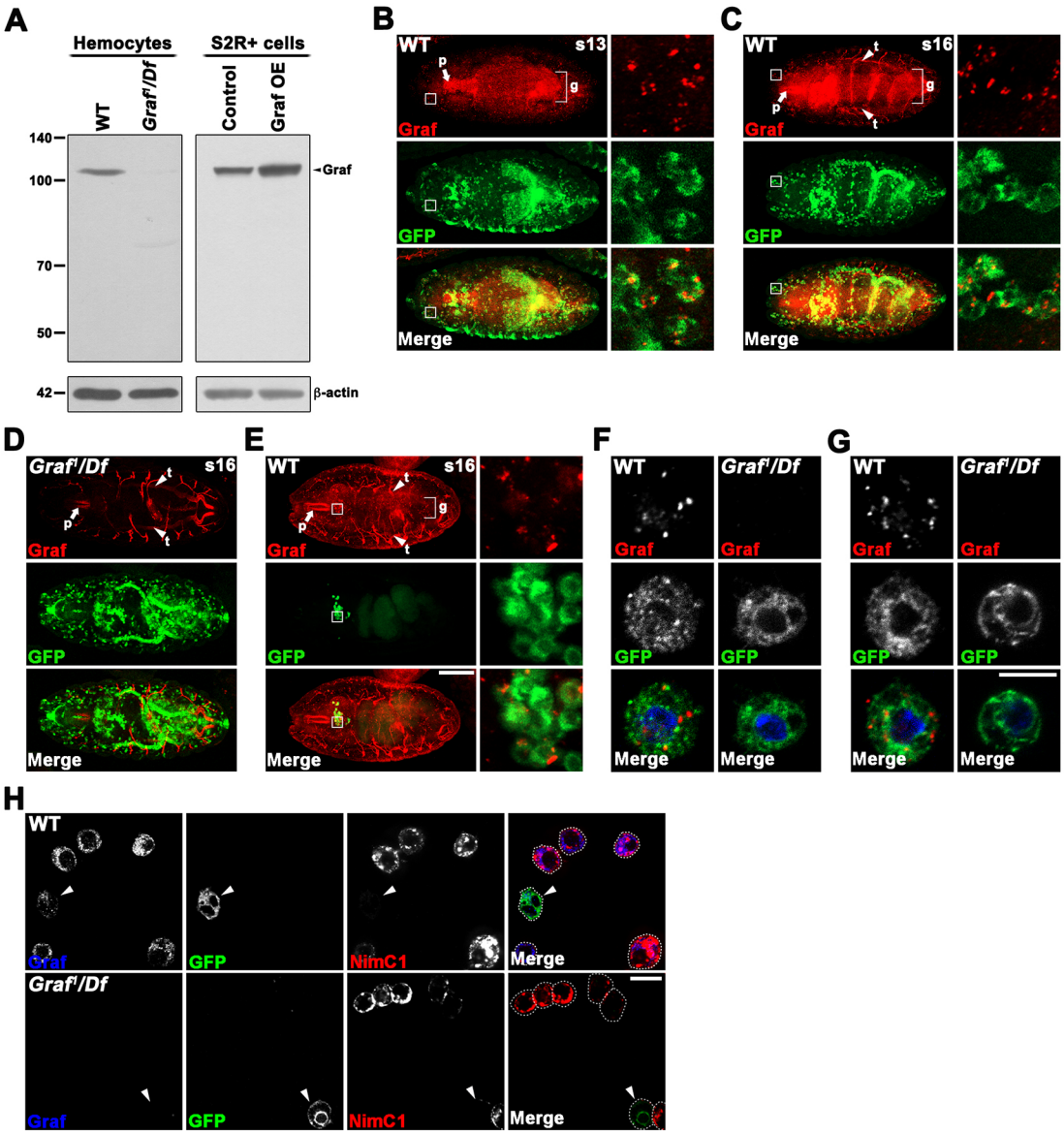

Fig. 2. Expression of Graf protein in *Drosophila* hemocytes. (A) Western blot analysis of extracts from third instar larval hemocytes [wild type (w^{1118}) or $Graf^{1}/Df$] and S2R+ cells (untreated or transfected with *UAS-Graf* and *actin 5C-GAL4*) using anti-Graf and anti-β-actin antibodies. Numbers on the left indicate molecular masses in kDa. (B-E) Confocal images of embryos stained using anti-Graf (red) and anti-GFP (green) antibodies. Dorsal views of projections through the whole embryo. Enlargements (single confocal sections) of the regions marked by boxes are shown on the right to highlight the punctate staining pattern of Graf. (B,C) Stage 13 (B) and 16 (C) wild-type embryos carrying *srp-GAL4* and *UAS-mCD8-GFP*. The anti-Graf signal is most prominent in migrating GFP-positive plasmatocytes, the gut (g, bracket), the trachea (t, arrowhead) and the pharynx (p, arrow). (D) A stage 16 $Graf^{1}/Df$ embryo carrying *srp-GAL4* and *UAS-mCD8-GFP*. Non-specific anti-Graf signal remains detectable in the trachea and pharynx. (E) A stage 16 wild-type embryo carrying *lz-GAL4* and *UAS-mCD8-GFP*. Anti-Graf signals are clearly detectable in GFP-positive crystal cells clustered around the proventriculus. (F,G) Single confocal sections of hemocytes from stage 16 wild-type and $Graf^{1}/Df$ embryos carrying *srp-GAL4*/*UAS-mCD8-GFP* (F) or *lz-GAL4*/*UAS-mCD8-GFP* (G). Hemocytes were stained with anti-Graf (red) and anti-GFP (green) antibodies. Nuclei were visualized by DAPI (blue) staining to highlight the cytoplasmic distribution of Graf-positive puncta. (H) Single confocal sections of circulating hemocytes from wild-type (top) or $Graf^{1}/Df$ (bottom) third instar larvae carrying *lz-GAL4* and *UAS-mCD8-GFP*. Hemocytes were bled and stained with anti-Graf (blue) and anti-NimC1 (red) antibodies. GFP expression is shown in green. Graf-positive puncta appear in NimC1-positive, GFP-negative plasmatocytes and NimC1-negative, GFP-positive crystal cells (arrowheads). Scale bars: 100 µm in E for B-E; 5 µm in G; 10 µm in H.

embryonic crystal cells, we also performed a similar experiment with wild-type and $Graf^{1}/Df$ embryos expressing *UAS-mCD8-GFP* under the control of the crystal cell-specific *lozenge* (*lz*)-*GAL4* driver (Lebestky et al., 2000). We observed punctate anti-Graf signal in Lz-GFP^{+} crystal cells clustered around the proventriculus of wild-type but not $Graf^{1}/Df$ embryos (Fig. 2E and data not shown). Finally, to further assess the subcellular localization of Graf puncta, we analyzed GFP-positive hemocytes isolated from embryos carrying *UAS-mCD8-GFP* and *srp-GAL4* or *lz-GAL4*. Additional nuclear staining with DAPI clearly revealed that Graf puncta had a cytoplasmic distribution in Srp-GFP^{+} and Lz-GFP^{+} hemocytes (Fig. 2F,G).

Next, we explored Graf expression in the larval hematopoietic system. To do this, we doubly stained hemocytes from wild-type and $Graf^{1}/Df$ third instar larvae carrying both *lz-GAL4* and *UAS-mCD8-GFP* with anti-Graf and an antibody against plasmatocyte-specific Nimrod C1 (NimC1). We found that Graf was expressed in a punctate pattern in most NimC1^{+} plasmatocytes and Lz-GFP^{+}

Development (2017) 144, 4159-4172 doi:10.1242/dev.153288

crystal cells from wild-type larvae (Fig. 2H). Anti-Graf signal was dramatically decreased in NimC1^{+} or Lz-GFP^{+} hemocytes from *Graf^{1}/Df* larvae (Fig. 2H). We also observed specific Graf expression throughout the medullary and cortical zones of the primary LG lobe but not in the posterior signaling center (PSC) (Fig. S1).

Graf restrains plasmatocyte proliferation by inhibiting the EGFR-Ras-MAPK pathway

To assess the role of Graf in the regulation of hematopoiesis, we compared hemocyte levels in wild-type and *Graf^{1}/Df* third instar larvae. We found approximately threefold higher levels of circulating and total (i.e. circulating plus sessile) hemocytes in *Graf^{1}/Df* larvae than in wild-type controls (Fig. 3A,B; Fig. S2A). Using the hemocyte reporter *HmlΔ-DsRed* (Makhijani et al., 2011), we confirmed that the sessile compartment of *Graf^{1}/Df* larvae also contains increased levels of hemocytes (Fig. 3C). Finally, *Graf^{1}/Df* larvae had 30% more hemocytes in the primary LG lobe (Fig. S2B). Thus, hemocyte numbers are increased in all hematopoietic compartments of *Graf* mutant larvae.

We were able to ascribe the increase in the larval hemocytes to a lineage-specific increase in plasmatocytes rather than other hemocyte types. First, *Graf^{1}/Df* larvae displayed a threefold increase in the concentration of circulating hemocytes labeled by the plasmatocyte lineage marker *crq-GAL4, UAS-mCD8-GFP* (Fig. 3D). However, loss of Graf did not significantly alter the concentration of circulating hemocytes labeled by the crystal cell lineage marker *lz-GAL4, UAS-mCD8-GFP* (Fig. 3D). Second, *Graf^{1}/Df* larvae had similar numbers of sessile crystal cells as wild-type larvae (Fig. S2C). Third, the percentage of lamellocytes, marked by the L1 antigen, was not significantly different between wild-type and *Graf^{1}/Df* mutant larvae (wild type, 0.1±0.01%; *Graf^{1}/Df*, 0.15±0.03%; P=0.11). Finally, plasmatocyte-specific expression of *UAS-Graf-HA* using *crq-GAL4* fully rescued the hemocyte overproduction phenotype of *Graf^{1}/Df* larvae (Fig. 3B; Fig. S2A).

To confirm the cell type-specific effect of Graf on hematopoiesis, we stained primary LG lobes for NimC1, Lz, L1 and the PSC marker Antennapedia (Antp). Compared with wild-type controls, *Graf^{1}/Df* mutants show a significant increase in the proportion of

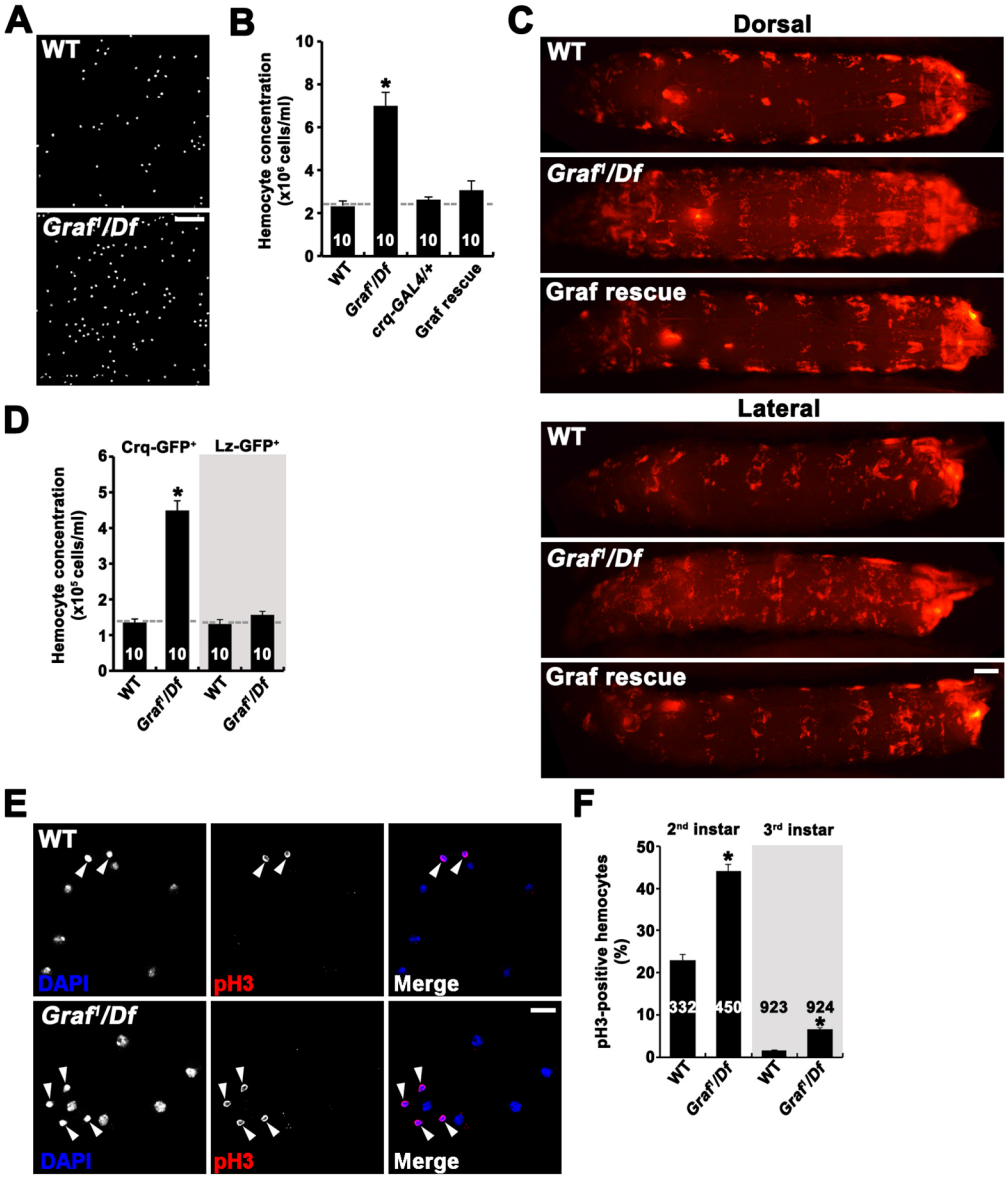

Fig. 3. Loss of Graf results in plasmatocyte overproliferation. (A) Representative confocal images of hemolymph smears from wild-type (*w^{1118}*) and *Graf^{1}/Df* third instar larvae. Each hemolymph sample was mixed with an equal volume of DAPI solution to visualize hemocyte nuclei. (B) Concentration of circulating hemocytes in third instar larvae of the following genotypes: wild type, *Graf^{1}/Df*, *crq-GAL4/+* and *Graf^{1}/Df*; *crq-GAL4/+*; *+/UAS-Graf-HA* (Graf rescue). (C) Live mount images of wild-type, *Graf^{1}/Df* and *Graf^{1},srp-GAL4/Df*; *+/UAS-Graf-HA* (Graf rescue) third instar larvae expressing *HmlΔdsRed*. (D) Concentration of circulating GFP-positive hemocytes in *UAS-mCD8-GFP/+*; *crq-GAL4/+* (Crq-GFP^{+} WT), *Graf^{1},+/Df,UAS-mCD8-GFP*; *crq-GAL4/+* (Crq-GFP^{+} *Graf^{1}/Df*), *lz-GAL4/UAS-mCD8-GFP* (Lz-GFP^{+} WT) and *Graf^{1},lz-GAL4/Df,UAS-mCD8-GFP* (Lz-GFP^{+} *Graf^{1}/Df*) third instar larvae. (E,F) *Graf* mutants show an excess of pH3-positive cells. (E) Confocal images of total (circulating and sessile) hemocytes from wild-type and *Graf^{1}/Df* second instar larvae [68-72 h after egg laying (AEL)], stained with DAPI and an anti-phospho-histone H3 (pH3) antibody (arrowheads). (F) Percentage of pH3-positive hemocytes among total hemocytes is shown for the second (68-72 h AEL) and third (92-96 h AEL) instar larvae. Data are mean±s.e.m. The total number of hemolymph samples (B,D; five independent experiments) or hemocytes (F; three independent experiments) analyzed is indicated within each bar. Each hemolymph sample involves five larvae. Comparisons are made against wild type (*P<0.001). Scale bars: 50 µm in A; 200 µm in C; 10 µm in E.

Development (2017) 144, 4159-4172 doi:10.1242/dev.153288

NimC1$^+$ plasmatocytes in the primary LG (Fig. S2D). However, the populations of Lz$^+$ crystal cells and Antp$^+$ PSC cells were not affected in the *Graf* mutants (Fig. S2E,F). Moreover, as in wild type, the number of L1$^+$ lamellocytes per lobe remained low in *Graf*^{1}*/Df* mutant larvae (wild-type, 0.8±0.27; *Graf*^{1}*/Df*, 0.9±0.22; P=0.77). Thus, hemocyte overproduction in the *Graf* mutant LG is also due to a selective increase in the plasmatocyte population.

We next asked whether this *Graf* phenotype is due to an increase in hemocyte proliferation. Staining total hemocytes using an anti-phospho-histone H3 (pH3) antibody revealed a significantly higher proportion of mitotically active (pH3-positive) hemocytes in *Graf*^{1}*/Df* larvae than in wild-type controls (1.9- and 4.2-fold in second and third instar larvae, respectively; Fig. 3E,F). We also quantified hemocyte proliferation using S/G2/M-Green fucci, a fluorescent ubiquitylation-based cell cycle indicator (Makhijani et al., 2011; Sakaue-Sawano et al., 2008). Indeed, *Graf* mutations increased the proportion of fucci-positive hemocytes to a similar extent (1.7- and 2.6-fold in second and third instar larvae, respectively; Fig. S2G,H). Thus, the overabundance of plasmatocytes in *Graf* mutants can be attributed primarily to increased cellular proliferation.

Elevated EGFR/Ras/MAPK signaling has been shown to cause plasmatocyte overproliferation without affecting other hemocyte lineages (Zettervall et al., 2004). We therefore hypothesized that the plasmatocyte overproliferation phenotype of *Graf*-null mutants was associated with abnormal EGFR signaling. To test this, we first examined levels of EGFR and its downstream signaling components in primary *Graf*^{1}*/Df* hemocytes. Staining with an anti-EGFR antibody revealed upregulation of EGFR expression in *Graf*^{1}*/Df* hemocytes compared with wild-type controls (Fig. 4A,B). We also observed parallel elevation of MAPK activation by staining for diphospho-ERK (dp-ERK), a downstream target of EGFR signaling (Fig. 4A,B). In sharp contrast, levels of phospho-AKT (p-AKT), another downstream target, remained normal (Fig. 4B). We confirmed this selective increase in dp-ERK in *Graf* mutants by western blot analysis of larval extracts (Fig. 4C,D). Thus, *Graf* mutant hemocytes display aberrant upregulation of EGFR/MAPK signaling.

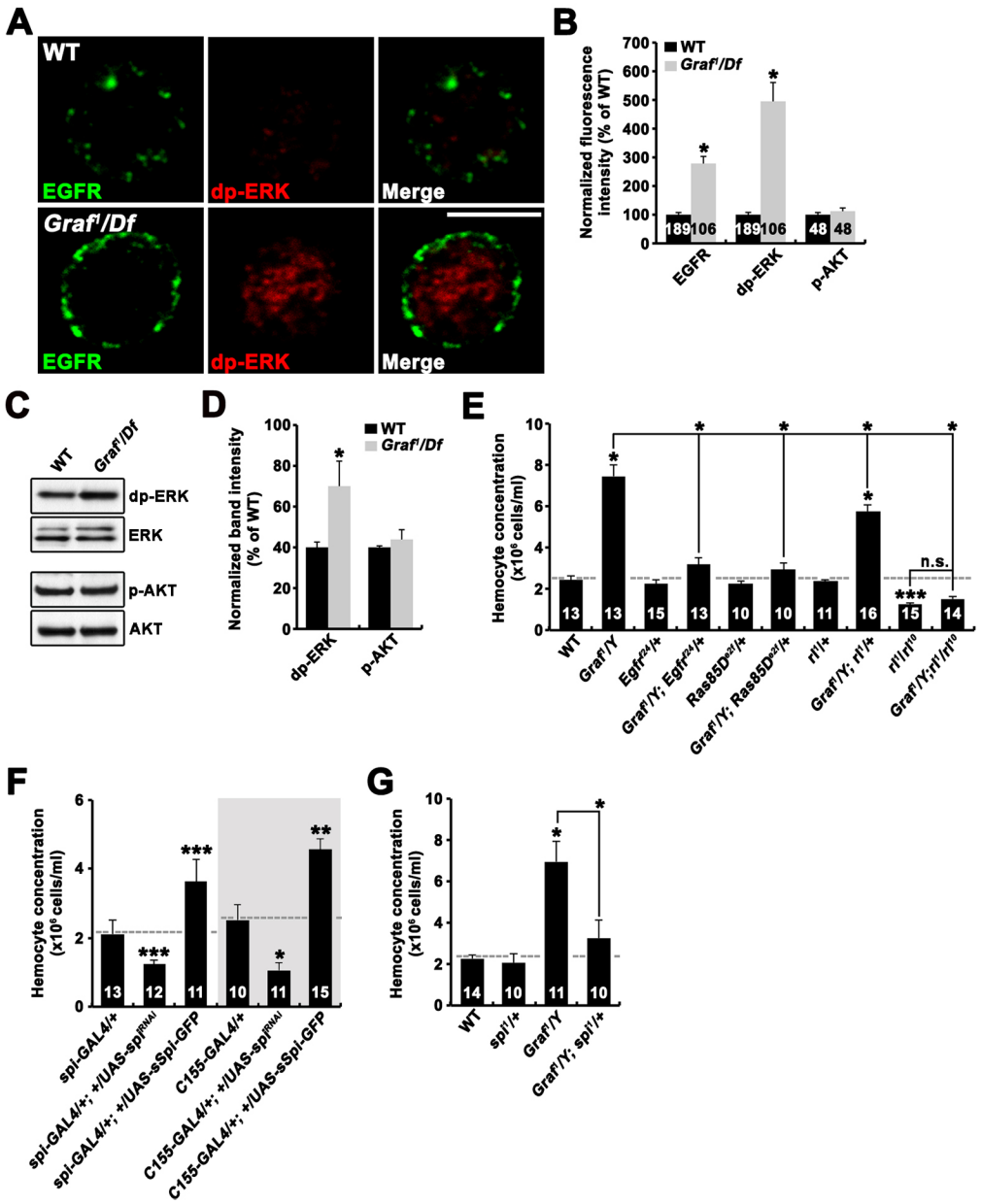

Fig. 4. Graf regulates EGFR-dependent plasmatocyte development. (A-D) *Graf* mutant hemocytes show increased levels of EGFR signaling. (A) Single confocal sections of hemocytes from wild-type (w^{1118}) and *Graf*^{1}*/Df* embryos stained for EGFR (green) and dp-ERK (red). (B) The ratio of mean EGFR, dp-ERK or phospho-AKT (p-AKT) to DAPI fluorescence intensities. (C) Western blot analysis of larval extracts prepared from wild-type and *Graf*^{1}*/Df* third instar larvae, using anti-dp-ERK, anti-ERK, anti-p-AKT and anti-AKT antibodies. (D) Normalized ratios of dp-ERK to total ERK and p-AKT to AKT from three separate western blots as measured by densitometry (n=3). (E-G) Concentration of circulating larval hemocytes is shown for the indicated genotypes. (E) Hemocyte overproduction in *Graf* is sensitive to EGFR/Ras/MAPK signaling levels. (F) Spi stimulates hemocyte production. (G) Hemocyte overproduction in *Graf* is sensitive to Spi levels. Values are mean±s.e.m. The total number of hemocytes (B; three independent experiments) or hemolymph samples (E-G; five independent experiments) analyzed is indicated within each bar. Each hemolymph sample involves five larvae. Comparisons are made against wild type (B,E,G) or an appropriate GAL4 control (F) unless otherwise indicated (*P<0.001; **P<0.01; ***P<0.05; n.s., not significant). Scale bar: 5 µm.

Development (2017) 144, 4159-4172 doi:10.1242/dev.153288

We next looked for genetic interactions between *Graf* and components of the EGFR signaling pathway. Loss of one copy of *Egfr*, *Ras85D/Ras1* or the MAPK gene *rolled* (*rl*) did not affect the level of circulating hemocytes in the wild-type background, but partially or completely suppressed the hemocyte overproduction observed in *Graf* mutants (Fig. 4E). Moreover, hemocyte overproduction in *Graf* was further suppressed by removing both copies of *rl* (Fig. 4E). These data indicate that hemocyte overproduction in *Graf* requires EGFR signaling and further that Graf restrains plasmatocyte proliferation by inhibiting EGFR signaling.

Finally, we examined genetic interactions between *Graf* and *spi*, the latter which encodes the principal ligand for EGFR in most tissues (Rutledge et al., 1992). In a control experiment, we first examined the role of Spi in hemocyte development. Overexpression of *UAS-sSpi-GFP* (i.e. a secreted Spi::GFP fusion protein) using *spi-GAL4* or the pan-neuronal driver *C155-GAL4* potently increased hemocyte production (Fig. 4F), phenocopying EGFR gain of function (Zettervall et al., 2004). In contrast, expression of *UAS-spi*^{RNAi} with the same GAL4 drivers had the opposite effect, mimicking the *rl* mutation (Fig. 4F). Importantly, loss of one copy of *spi*, which had no effect on hemocyte abundance alone, fully suppressed the hemocyte overproduction observed in *Graf* mutants (Fig. 4G). These results indicate that hemocyte overproduction in *Graf* requires EGFR activation.

Graf-dependent GEEC endocytosis is essential for EGFR degradation

Mammalian GRAF1 is an essential component of the GEEC endocytic pathway (Lundmark et al., 2008). We confirmed that this role is conserved in *Drosophila* Graf. Not only was Graf prominently localized to CLIC/GEEC endocytic membranes in *Drosophila* primary hemocytes and S2R+ cells (Fig. S3A-G), but Graf was also required for efficient fluid-phase uptake (Fig. S3H,I).

How does the endocytic protein Graf attenuate EGFR activation? In a variety of mammalian cells, low EGF (≤2 ng/ml) treatment causes clathrin-dependent (CD) endocytosis of EGFR and subsequently its recycling to the plasma membrane, whereas high EGF also induces clathrin-independent (CI) endocytosis and degradation of the receptor (Sigismund et al., 2008, 2005). We therefore hypothesized that Graf-dependent GEEC endocytosis plays an important role in endocytic downregulation of EGFR under conditions of high EGF. To test this, we used several approaches.

We first examined the role of GEEC endocytosis in internalizing EGFR at low and high Spi. To do so, we stimulated primary larval hemocytes with 4 or 30 ng/ml sSpi-GFP (i.e. ∼1.3 or 10 ng/ml sSpi) and quantified the amount of ligand internalized for up to 2 min by anti-GFP immunostaining. The amount of internalized ligand in wild-type hemocytes stimulated with high sSpi-GFP was significantly greater than in wild-type hemocytes stimulated with low sSpi-GFP (Fig. 5A,B). Importantly, loss of Graf or knockdown of Arf1 and Arf-GEF (guanine nucleotide exchange factor) Garz, two well-established regulators of GEEC endocytosis (Gupta et al., 2009; Kumari and Mayor, 2008), reduced ligand internalization by ∼36-50% under high sSpi-GFP, but had no effect under low sSpi-GFP (Fig. 5B). In sharp contrast, knockdown of clathrin heavy chain (Chc) strongly impaired ligand internalization only under low sSpi-GFP (Fig. 5B). Finally, consistent with a previous report demonstrating that GEEC endocytosis in hemocytes is dynamin independent (Guha et al., 2003), treatment of hemocytes with dynasore did not affect sSpi-GFP internalization under high sSpi-GFP. In control experiments, dynasore treatment strongly impaired ligand internalization under low sSpi-GFP (Fig. 5B). Collectively, these results demonstrate that ligand-activated EGFR can be internalized via both CD and GEEC endocytosis and that high Spi stimulation skews the partitioning of EGFR endocytosis toward the latter route.

To corroborate the above conclusions, we treated primary wild-type hemocytes with low or high sSpi-GFP and visualized the early steps of ligand internalization compared with endogenous Graf and Chc. Immediately after low sSpi-GFP stimulation (2 min), the internalized ligand appeared intracellularly in a punctate pattern and these puncta colocalized more extensively with Chc than with Graf (27% versus 9%, respectively; Fig. 5D). However, under high sSpi-GFP conditions, the internalized ligand showed the opposite behavior (13% with Chc versus 30% with Graf; Fig. 5C,D), supporting that high Spi stimulation skews the partitioning of EGFR endocytosis toward the GEEC pathway.

We then examined the effect of high Spi treatment on GEEC endocytosis-mediated fluid phase uptake. We pretreated primary hemocytes from wild-type larvae with both FITC-labeled dextran (FITC-Dex; a GEEC endocytosis marker) and low or high sSpi-GFP at 4°C for 30 min and subsequently allowed uptake of FITC-Dex at 25°C for 2 min. Both the total amount of FITC-Dex internalized and the number of intracellular puncta double positive for Graf and FITC-Dex in high Spi-treated hemocytes were not significantly different from those observed in low Spi-treated hemocytes (Fig. 5E,F), indicating that high Spi induces GEEC endocytosis of EGFR without affecting the activity of the GEEC pathway.

Next, we investigated whether GEEC endocytosis is associated with efficient sorting of internalized EGFR to lysosomes. We treated primary larval hemocytes with low or high Spi and visualized ligand internalized for up to 30 min in comparison with the lysosome marker Lysotracker. The extent of sSpi-GFP-Lysotracker colocalization in wild-type hemocytes treated with high sSpi-GFP was significantly greater than in wild-type hemocytes treated with low sSpi-GFP (51% versus 17%; Fig. 5G,H). This high Spi-induced effect was strongly abolished by loss of Graf, Arf1 or Garz but not by loss of Chc. In control experiments, malelylated bovine serum albumin (a CD endocytosis marker) was normally internalized and targeted to lysosomes in *Graf* mutant hemocytes under high Spi (data not shown), confirming that the effect of interfering GEEC endocytosis is not due to global defects in endocytic protein trafficking to lysosomes. Under low sSpi-GFP, loss of Chc resulted in a small but significant reduction in sSpi-GFP-Lysotracker colocalization, whereas loss of Graf, Arf1 or Garz had no effect (Fig. 5H). Thus, GEEC endocytosis, but not CD endocytosis, of EGFR is associated with its efficient sorting to lysosomes.

Finally, we directly investigated the impact of GEEC endocytosis on EGFR degradation at high Spi. When S2R+ cells overexpressing Flag-EGFR were stimulated with 30 ng/ml sSpi-GFP, we observed robust Flag-EGFR degradation and enhanced MAPK activation beginning within 5 min that was almost completely abolished by 60 min (Fig. 5I,J). However, loss of Graf or Arf1, but not Chc, strongly impaired ligand-induced Flag-EGFR degradation, leading to more sustained activation of ERK (Fig. 5I,J). Thus, GEEC endocytosis, but not CD endocytosis, of EGFR is indispensable for its efficient degradation under the condition of high Spi.

D-Cbl-mediated ubiquitylation of EGFR is required for its GEEC endocytosis and normal plasmatocyte proliferation

In mammalian cells, CI endocytosis of EGFR at high EGF requires its ubiquitylation (Sigismund et al., 2013, 2005), which is mediated

Development (2017) 144, 4159-4172 doi:10.1242/dev.153288

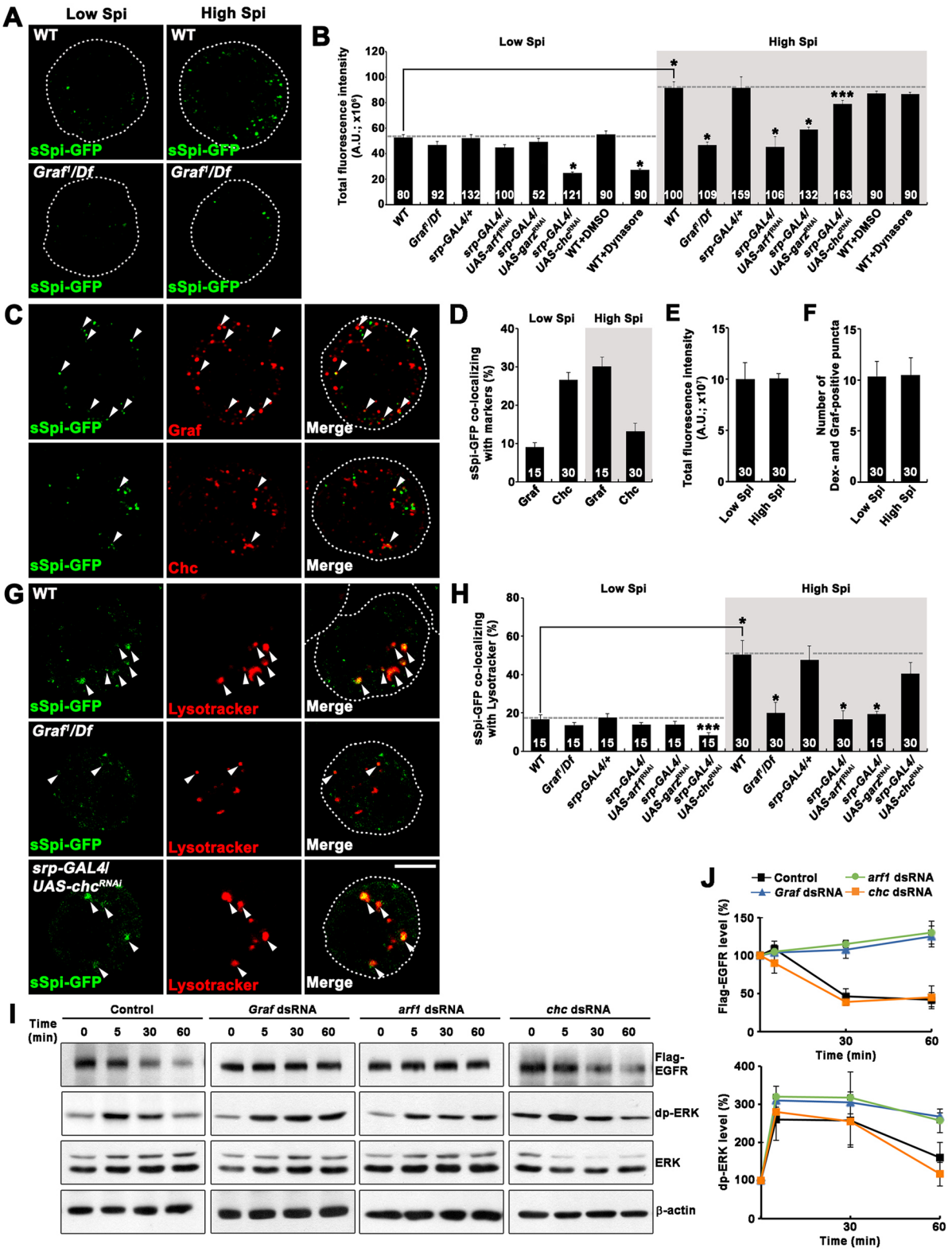

Fig. 5. See next page for legend.

by the E3 ligase Cbl (Levkowitz et al., 1999, 1998). To investigate the mechanistic link between EGFR ubiquitylation and GEEC endocytosis, we initially assessed the extent of receptor ubiquitylation in S2R+ cells stimulated with either low or high Spi. EGFR ubiquitylation was detected only under high Spi, as demonstrated by immunoblotting using the P4D1 antibody that recognizes ubiquitin (Ub) monomers and polymers (Fig. S4A). Given the effect of high Spi on GEEC endocytosis, this result establishes a positive correlation between EGFR ubiquitylation and GEEC endocytosis of the receptor.

Development (2017) 144, 4159-4172 doi:10.1242/dev.153288

Fig. 5. Graf-dependent GEEC endocytosis is required for EGFR internalization and degradation at high Spi. (A,B) Loss of Graf or Arf1 strongly reduces total EGFR internalization under high Spi. (A) Primary hemocytes from wild-type (w^{1118}) or $Graf^{1}/Df$ third instar larvae were stained with anti-GFP antibody after being pretreated with conditioned medium containing low or high sSpi-GFP (4 or 30 ng/ml, respectively) at 4°C for 30 min and then incubated with serum-free medium lacking sSpi-GFP at 25°C for 2 min. Single confocal sections through the middle of cells are shown. (B) Quantification of the amount of internalized sSpi-GFP in primary hemocytes of the indicated genotypes from experiments performed in A. In some experiments, wild-type hemocytes were treated with DMSO or 20 µM dynasore for 30 min before addition of sSpi-GFP. Total GFP fluorescence intensity per cell was determined (A.U., arbitrary units). (C,D) High Spi induces GEEC endocytosis of EGFR. (C) Primary hemocytes from wild-type third instar larvae were immunostained for GFP (green) and endogenous Graf or Chc (red) after being stimulated with high sSpi-GFP as in A. Single confocal sections through the middle of cells are shown. Arrowheads indicate intracellular puncta labeled for both sSpi-GFP and Graf or Chc. (D) Quantification of sSpi-GFP-Graf colocalization. (E,F) Fluid-phase uptake in primary larval hemocytes is not significantly different at low and high Spi. Primary wild-type hemocytes were incubated with both FITC-Dex and low or high sSpi-GFP at 4°C for 30 min. Following a 2 min incubation at 25°C, cells were stained for endogenous Graf. (E) Quantification of the amount of internalized FITC-Dex. Total green fluorescence intensity per cell was determined. (F) Quantification of the number of intracellular puncta labeled with both Graf and FITC-Dex. (G,H) GEEC endocytosis is required for efficient lysosomal targeting of internalized EGFR at high Spi. (G) Primary hemocytes from wild-type, $Graf^{1}/Df$ or *srp-GAL4/UAS-chc*^{RNAi} third instar larvae were pretreated with sSpi-GFP as in A and then incubated at 25°C for 25 min. Cells were then treated with 1 µM Lysotracker (red) at 25°C for 5 min prior to staining for GFP (green). Single confocal sections through the middle of cells are shown. Arrowheads indicate intracellular puncta labeled for sSpi-GFP and Lysotracker. (H) Quantification of sSpi-GFP-Lysotracker colocalization in primary hemocytes of the indicated genotypes from experiments performed as in G. (I,J) GEEC endocytosis is associated with efficient EGFR degradation at high Spi. (I) Western blot analysis of total lysates of S2R+ cells transfected with *actin 5C-GAL4* and *UAS-Flag-Egfr* with or without the indicated dsRNA. Cells were pretreated with 100 µg/ml cycloheximide for 3 h to inhibit new protein synthesis and then further incubated in the presence of 30 ng/ml sSpi-GFP at 25°C for the indicated times. (J) Quantification of Flag-EGFR (left) or dp-ERK (right) normalized to β-actin or total ERK, respectively. Mean values from three independent experiments are plotted against incubation time. Data are mean ±s.e.m. The number of hemocytes analyzed in three independent experiments is indicated within each bar. Comparisons are made against low or high Spi-treated wild-type hemocytes unless otherwise indicated (*P<0.001; ***P<0.05). Scale bar: 5 µm.

We then analyzed the relevance of *Drosophila* Cbl (D-Cbl) to GEEC endocytosis of EGFR. For this, we prepared primary hemocytes from larvae carrying a hypomorphic *D-cbl* mutation ($D\text{-}cbl^{KG03080}$) and stimulated them for 2 min with high Spi (i.e. 30 ng/ml sSpi-GFP). The amount of internalized sSpi-GFP in $D\text{-}cbl^{KG03080}$ hemocytes was decreased by 37% compared with control *crq-GAL4/+* hemocytes (Fig. 6A,B). Importantly, this defect was concurrent with a substantial decrease in sSpi-GFP-Graf colocalization (18% in $D\text{-}cbl^{KG03080}$ versus 31% in *crq-GAL4/+*; Fig. 6C,D), demonstrating a reduction in sSpi-GFP internalization via GEEC endocytosis. Expression of the longer isoform of D-Cbl (D-CblL) in $D\text{-}cbl^{KG03080}$ hemocytes simultaneously increased sSpi-GFP internalization and sSpi-GFP-Graf colocalization to control levels, while similar expression of an E3 ligase-defective D-CblLΔ70Z mutant did not (Fig. 6B,D). These results support the importance of the E3 ligase activity of D-Cbl for GEEC endocytosis of EGFR.

Next, we directly assessed the role of D-Cbl-mediated receptor ubiquitylation in GEEC endocytosis of EGFR. To do so, we first demonstrated that the Y1271F point mutation in EGFR significantly impaired its ability to recruit D-Cbl and undergo ubiquitylation in response to high Spi (Fig. S4B-E). We then examined the impact of this mutation on the GEEC endocytosis of EGFR. S2R+ cells expressing Flag-EGFR or Flag-EGFR-Y1271F in combination with exogenous GFP-GPI (a GEEC pathway marker) were analyzed for early trafficking steps of transfected EGFR protein. After prelabeling surface Flag-EGFR and GFP-GPI with anti-Flag and anti-GFP antibodies at 4°C, we stimulated cells with high sSpi-HA (10 ng/ml) at 25°C for 2 min to allow Flag-EGFR endocytosis. A major fraction (~66%) of the internalized Flag-EGFR pool colocalized with GFP-GPI-containing endosomes, whereas only 24% of internalized Flag-EGFR-Y1271F receptors did so (Fig. S4F, G). We also examined the impact of the Y1271F mutation on EGFR degradation. Under high sSpi-HA, Flag-EGFR-Y1271F showed less degradation than wild-type Flag-EGFR (Fig. S4H,I), confirming the notion that GEEC endocytosis of EGFR is indispensable for efficient receptor degradation. Thus, D-Cbl-mediated ubiquitylation of EGFR is required for its GEEC endocytosis and subsequent degradation.

To investigate the *in vivo* role of D-Cbl in downregulating EGFR, we first examined hemocyte development in $D\text{-}cbl^{KG03080}$ mutants. We found significantly higher levels of circulating hemocytes in homozygous $D\text{-}cbl^{KG03080}$ larvae than in wild-type larvae (Fig. 6E, F). In addition, $D\text{-}cbl^{KG03080}$ larvae showed a 1.8-fold increase in the fraction of pH3-positive hemocytes (Fig. 6G). Plasmatocyte-specific expression of D-CblL, but not D-CblLΔ70Z, rescued the hemocyte overproduction observed in $D\text{-}cbl^{KG03080}$ mutants (Fig. 6F), underscoring the importance of the E3 ligase activity of D-Cbl in regulating plasmatocyte proliferation. As an additional approach, we also examined genetic interactions between *D-cbl* and *Egfr* (Fig. 6H). Plasmatocyte-specific overexpression of EGFR induced hemocyte overproliferation. Importantly, this phenotype was strongly suppressed by overexpressing D-Cbl, which had no effect on plasmatocyte proliferation in the wild-type background. In contrast, overexpression of D-CblLΔ70Z failed to suppress the EGFR overexpression phenotype. These results clearly establish a role for the E3 ligase activity of D-Cbl in EGFR downregulation during plasmatocyte development.

Ubiquitin-dependent interactions of EGFR with Graf

To further understand the mechanism underlying GEEC-mediated EGFR internalization, we first tested whether Graf interacts physically with EGFR. In GST pull-down experiments, GST-Graf, but not GST alone, precipitated Flag-EGFR from S2R+ cell lysates (Fig. 7A). We were also able to co-immunoprecipitate Flag-EGFR and endogenous Graf from S2R+ cell lysates using an anti-Flag antibody (Fig. 7B,C). Importantly, the EGFR-Graf interaction was enhanced by stimulating S2R+ cells with high sSpi-HA (Fig. 7A-C). This interaction was direct, as demonstrated by GST pull-down experiments using a GST fusion to the EGFR intracellular domain (GST-EGFR-IC) and purified His_6-Graf (Fig. 7D,E).

Next, we addressed the issue of whether D-Cbl-mediated EGFR ubiquitylation is required for the Spi-induced interaction of EGFR with Graf. We found that loss of D-Cbl, which had no effect on the basal EGFR-Graf interaction by itself, completely abolished the effect of high Spi treatment on the EGFR-Graf interaction (Fig. 7A-C). In addition, the Y1271F point mutation in EGFR also blocked the high Spi-induced EGFR-Graf interaction (Fig. 7A-C). Finally, the addition of a single ubiquitin molecule to GST-EGFR-IC enhanced its interaction with His_6-Graf (Fig. 7D,E). In a control experiment, GST-Ub, but not GST alone, also bound to His_6-Graf, revealing an intrinsic ability of Graf to bind Ub. These results

Development (2017) 144, 4159-4172 doi:10.1242/dev.153288

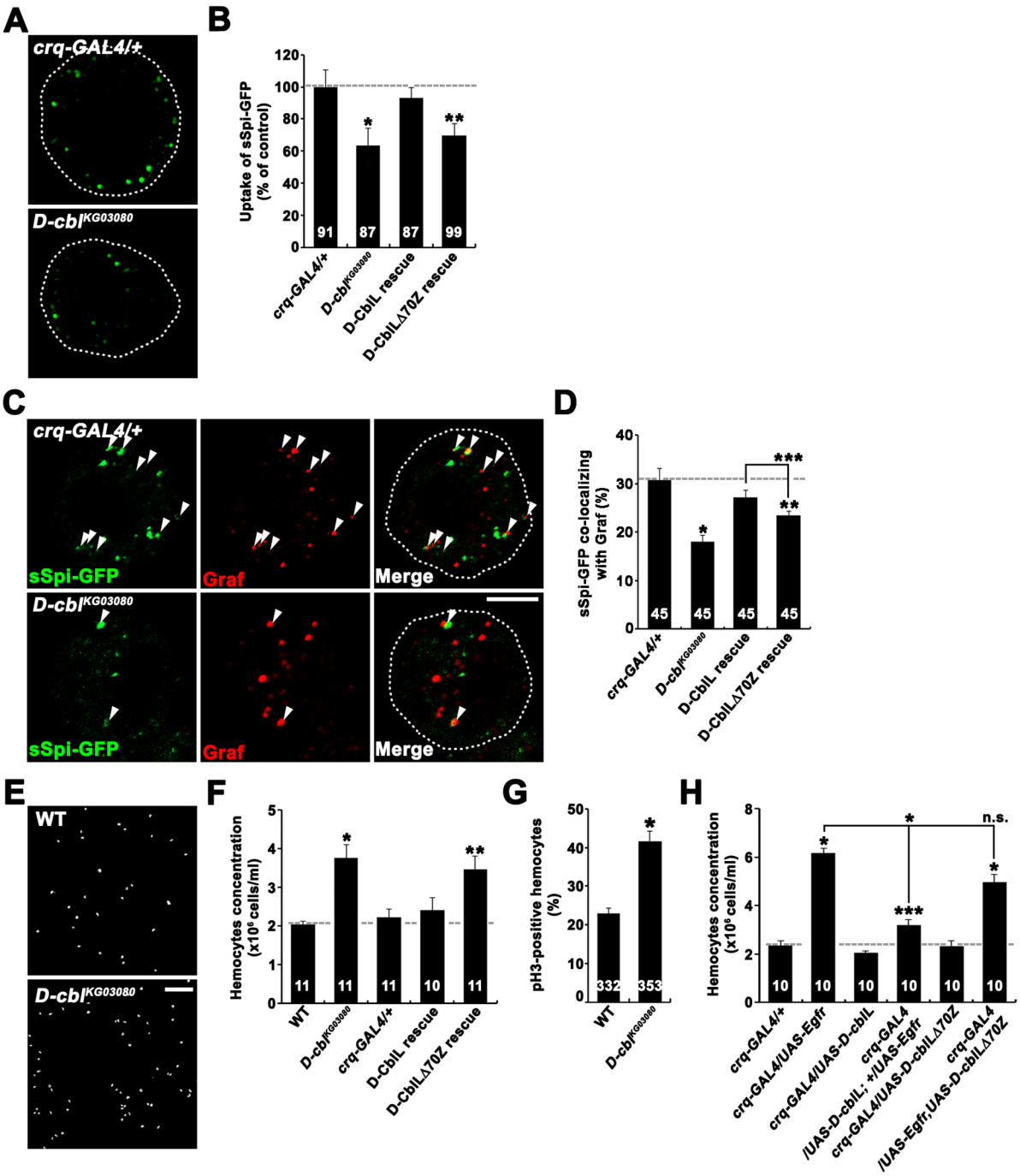

Fig. 6. D-Cbl is required for GEEC endocytosis of EGFR and normal hemocyte proliferation. (A,B) Loss of D-Cbl results in a significant reduction in total EGFR internalization at high Spi. (A) Primary hemocytes from *crq-GAL4*/+ (control) or *D-cbl*^{KG03080} third instar larvae were stained with an anti-GFP antibody after being pretreated with conditioned medium containing 30 ng/ml sSpi-GFP at 4°C for 30 min and then incubated with serum-free medium lacking sSpi-GFP at 25°C for 2 min. Single confocal sections through the middle of cells are shown. (B) Quantification of sSpi-GFP internalization in primary hemocytes of the following genotypes: *crq-GAL4*/+, *D-cbl*^{KG03080}/*D-cbl*^{KG03080}, *crq-GAL4*/*UAS-D-cblL*; *D-cbl*^{KG03080}/*D-cbl*^{KG03080} (D-CblL rescue) and *crq-GAL4*/+; *D-cbl*^{KG03080}/*D-cbl*^{KG03080},*UAS-D-cblLΔ70Z* (D-CblLΔ70Z rescue). (C,D) Loss of D-Cbl selectively impairs GEEC endocytosis of EGFR at high Spi. (C) Primary hemocytes from *crq-GAL4*/+ and *D-cbl*^{KG03080} third instar larvae were stained for GFP (green) and Graf (red) after being stimulated with sSpi-GFP as in A. Single confocal sections through the middle of cells are shown. Arrowheads indicate intracellular puncta labeled with both sSpi-GFP and Graf. (D) Quantification of sSpi-GFP-Graf colocalization in primary hemocytes from third instar larvae of the genotypes as in B. (E-H) D-Cbl controls EGFR-dependent hemocyte proliferation. (E) Confocal images of blood smears from wild-type (*w*^{1118}) and *D-cbl*^{KG03080} third instar larvae stained with DAPI. (F) Concentration of circulating hemocytes in wild-type third instar larvae and larvae of the genotypes as in B. (G) Percentage of pH3-positive hemocytes in the total (circulating and sessile) hemocyte population from wild-type and *D-cbl*^{KG03080} second instar larvae (68-72 h AEL). (H) Genetic interactions between *Egfr* and *D-cbl*. The concentration of circulating hemocytes is shown for third instar larvae of the indicated genotypes. Data are mean±s.e.m. The total number of analyzed hemocytes (B,D,G; three independent experiments) or hemolymph samples (F,H; five independent experiments) analyzed is indicated within each bar. Each hemolymph sample involves five larvae. Comparisons are made against *crq-GAL4*/+ (B,D,H) or wild type (F,G) unless otherwise indicated (*P<0.001; **P<0.01; ***P<0.05; n.s., not significant). Scale bars: 5 µm in C; 50 µm in E.

Development (2017) 144, 4159-4172 doi:10.1242/dev.153288

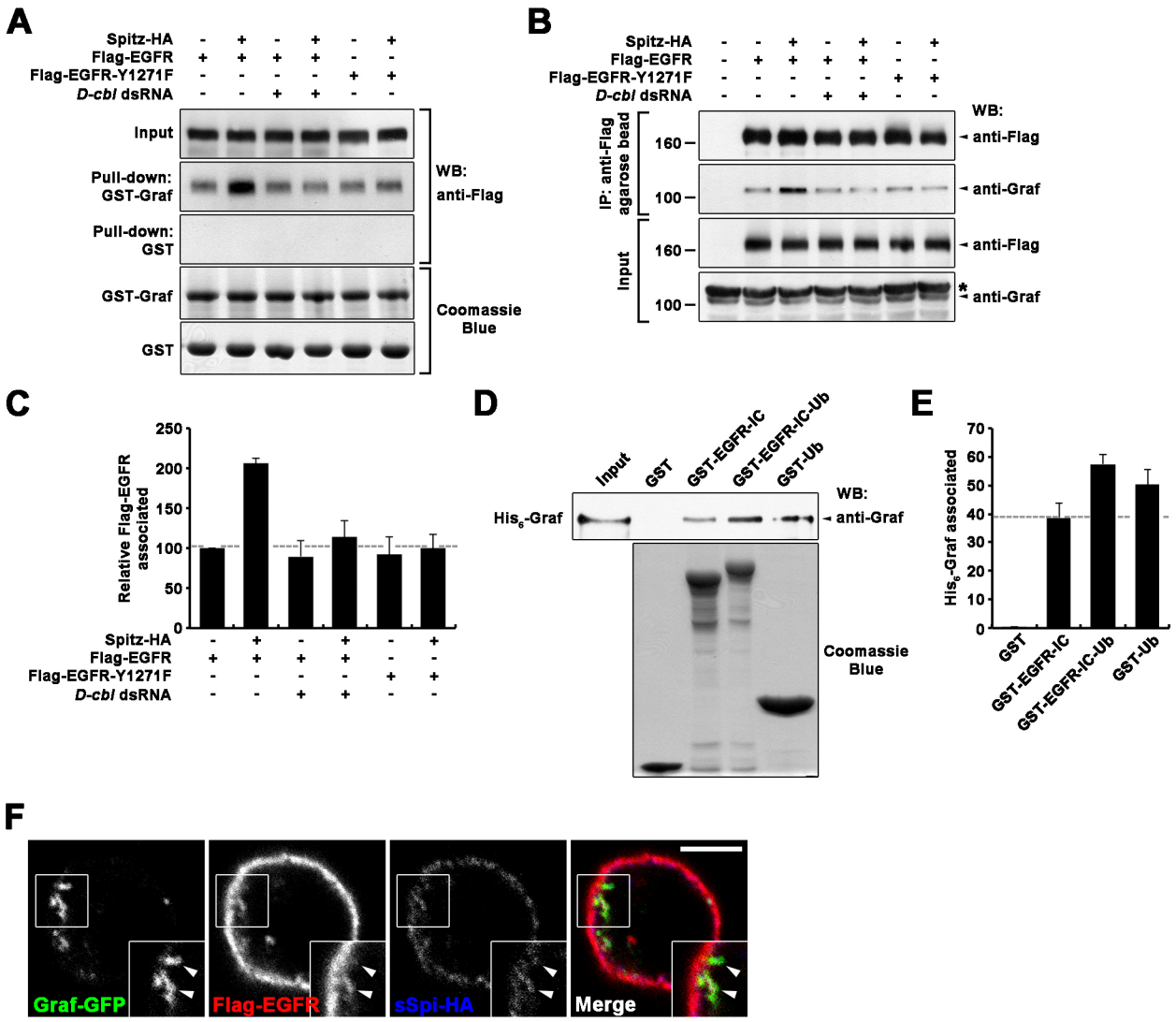

Fig. 7. High Spi enhances the interaction of EGFR with Graf by inducing D-Cbl-mediated EGFR ubiquitylation. (A-C) High Spi enhances EGFR-Graf interactions. S2R+ cells transfected with either Flag-EGFR or Flag-EGFR-Y1271F, with or without *D-cbl* dsRNA, were serum starved and stimulated with 10 ng/ml sSpi-HA for 5 min. Cell lysates were subjected to GST pull-down (A) and co-immunoprecipitation (B,C) experiments. (A) Western blot of cell lysates (input) or GST pull-downs probed with an anti-Flag antibody (three upper panels). The two lower panels show Coomassie Blue staining of GST-Graf and GST preparations. (B) Western blot of cell lysates (input) or anti-Flag immunoprecipitates probed with anti-Flag or anti-Graf antibody. (C) Quantification of Graf levels in anti-Flag immunoprecipitates by densitometry (n=3). (D,E) Ubiquitylation of EGFR-IC enhances its interaction with Graf. Purified recombinant His_6-Graf was incubated with GST, GST-EGFR-IC, GST-EGFR-IC-Ub or GST-Ub. (D) Western blot of GST pull-downs probed with anti-Graf antibody (upper panel). The lower panel shows Coomassie Blue staining of GST proteins. (E) Quantification of Graf levels in GST pull-downs by densitometry (n=3). (F) Graf and EGFR colocalize to internal structures derived from the plasma membrane. Live S2R+ cells expressing Myc-Cdc42Q61L, Graf-GFP and Flag-EGFR were serum-starved and incubated with anti-Flag antibodies at 4°C for 1 h to label Flag-EGFR on the cell surface. After subsequent incubation with 10 ng/ml sSpi-HA at 25°C for 2 min, cells were immunostained for Graf-GFP (green), Flag-EGFR (red) and sSpi-HA (blue). Single confocal sections through the middle of cells are shown. Arrowheads indicate cell surface-associated endocytic structures triply stained for Graf-GFP, Flag-EGFR and sSpi-HA. Scale bar: 10 µm.

support a model in which D-Cbl-mediated receptor ubiquitylation facilitates GEEC endocytosis of EGFR by promoting its physical interaction with Graf.

The above model predicts that Graf acts at the plasma membrane to recruit EGFR to GEEC endocytosis. However, in line with previous work demonstrating that the assembly of mammalian GRAF1 at the cell surface is very transient (Francis et al., 2015), Graf was barely detected at the cell surface in hemocytes and S2R+ cells (Fig. S3A-E). We therefore sought to stabilize the localization of Graf to nascent endocytic structures during EGFR internalization. To this end, we transfected S2R+ cells with Graf-GFP and Flag-EGFR in combination with a constitutively active Cdc42 mutant (Cdc42-Q61L), which has been shown to result in accumulation of assembled GRAF1 at the plasma membrane (Francis et al., 2015). Live cells were prelabeled for surface Flag-EGFR at 4°C and stimulated with high sSpi-HA at 25°C. After 2 min, the localization of Graf-GFP was visualized in comparison with that of internalized Flag-EGFR and sSpi-HA by immunocytochemistry. Under these conditions, Graf-GFP localized together with internalizing Flag-EGFR and sSpi-HA to punctate or tubular structures connected to the cell surface (Fig. 7F), supporting our conclusion that Graf recruits EGFR to GEEC endocytosis at the plasma membrane.

Development (2017) 144, 4159-4172 doi:10.1242/dev.153288

DISCUSSION

Deletions, truncations and mutations in the human *GRAF1* gene are associated with myeloid malignancies such as AML and MDS (Borkhardt et al., 2000; Panagopoulos et al., 2004; Wilda et al., 2005), but little is known about the role of GRAF family members in blood cell development. Here, we provide evidence that Graf, the only fly ortholog of mammalian GRAF proteins, acts cell-autonomously to regulate the proliferation of macrophage-like plasmatocytes. First, Graf is expressed in plasmatocytes. Second, *Graf* mutant larvae have more plasmatocytes than wild-type controls owing to increased cellular proliferation. Third, this *Graf* mutant phenotype is fully rescued by plasmatocyte-specific expression of Graf. Our data further imply that Graf restrains plasmatocyte proliferation by inhibiting the EGFR-Ras-MAPK pathway. Not only do *Graf* mutant hemocytes show elevated levels of EGFR and activated ERK, but hemocyte overproliferation in *Graf* mutants requires both the EGFR ligand Spi and the EGFR-Ras-MAPK cascade.

Unlike plasmatocytes, the populations of crystal cells and lamellocytes in both circulation and the LG are not significantly affected by loss of Graf. This finding is consistent with a previous report demonstrating that overexpression of wild-type EGFR in circulating hemocytes induces selective overproliferation of plasmatocytes without significantly affecting other hemocyte lineages (Zettervall et al., 2004). However, in another study, overexpression of a constitutively active *Egfr* mutant in both circulating hemocytes and the LG cortical zone was found to potently induce the generation of lamellocytes (Sinenko et al., 2011). The discrepancy with regard to lamellocyte differentiation could arise from differences in the timing and strength of signaling mediated by wild-type and constitutively active *Egfr* alleles. Another, not mutually exclusive, possibility is that discrete hemocyte populations respond to different thresholds of EGFR signaling activity.

Previous work has proposed that, upon parasitic infection, the PSC cells of the LG secrete Spi to induce lamellocyte differentiation in a non-cell-autonomous manner (Sinenko et al., 2011). However, it remains unknown whether the PSC cells also secrete Spi to induce plasmatocyte proliferation under normal developmental conditions. Our data raise the possibility that the nervous system is a physiological source of secreted Spi in the hemolymph. We find that pan-neuronal expression of Spi RNAi using *C155-GAL4* is sufficient to reduce hemocyte numbers in circulation. Conversely, expression of secreted Spi with the same driver has the opposite effect on hemocyte numbers in circulation. Furthermore, *spi-GAL4* is found to be highly active in a small subset of neurosecretory cells that innervate the ring gland, the major endocrine organ in *Drosophila* (S.K. and S.L., unpublished). It will be interesting in the future to determine whether the Spi section activity of the nervous system is controlled by developmental cues or infection.

Like human GRAF1, *Drosophila* Graf plays an important role in GEEC endocytosis. This raises the obvious issue of whether the two roles that Graf plays in regulating GEEC endocytosis and EGFR signaling are related. In mammalian cells, CI endocytosis of EGFR results in receptor degradation and signal attenuation in the presence of high ligand concentrations (Sigismund et al., 2008). Until now, the precise nature of the CI endocytic pathway mediating EGFR downregulation remained unclear. Here, we provide evidence that Graf-dependent GEEC endocytosis is a major CI endocytic route of EGFR internalization. Upon exposure to high concentrations of Spi, a substantial fraction of internalized Spi and EGFR colocalizes with Graf- or GFP-GPI-labeled CLICs/GEECs. Interfering with GEEC endocytosis by knocking down Graf or Arf1 strongly impairs this high-Spi-induced internalization of EGFR. We also provide evidence that GEEC endocytosis is essential for efficient EGFR degradation at high Spi. Loss of Graf or Arf1 significantly impairs high-Spi-induced EGFR degradation and signal attenuation. The EGFR-Y1271F mutant, which cannot be efficiently partitioned toward the GEEC pathway (see below), is much more resistant to high-Spi-induced degradation than wild-type EGFR. Our findings thus imply that Graf attenuates EGFR signaling by facilitating its GEEC endocytosis under conditions of high Spi (see Fig. 8).

In mammalian cells, ubiquitylation of EGFR by Cbl proteins seems to divert the receptor from CD to CI endocytosis at high EGF concentrations (Sigismund et al., 2013). Consistently, GEEC endocytosis of *Drosophila* EGFR also depends on Cbl-dependent receptor ubiquitylation. We find that high Spi treatment, which promotes the GEEC endocytosis of EGFR, potently induces EGFR ubiquitylation by the fly Cbl ortholog D-Cbl. In addition, the E3 ligase activity of D-Cbl is required for EGFR partitioning into the GEEC endocytic pathway. Furthermore, the ubiquitylation-defective EGFR-Y1271F mutant fails to undergo GEEC endocytosis at high Spi.

How are ubiquitylated EGFRs sorted preferentially to the GEEC endocytic pathway? We provide biochemical evidence that Graf itself participates in this sorting process via physical interactions with the ubiquitin (Ub) moiety on EGFR (Fig. 8). We show that Spi enhances the physical interactions of EGFR with Graf and that this enhancement requires D-Cbl recruitment to EGFR. We also show that the addition of a single Ub moiety to the EGFR intracellular

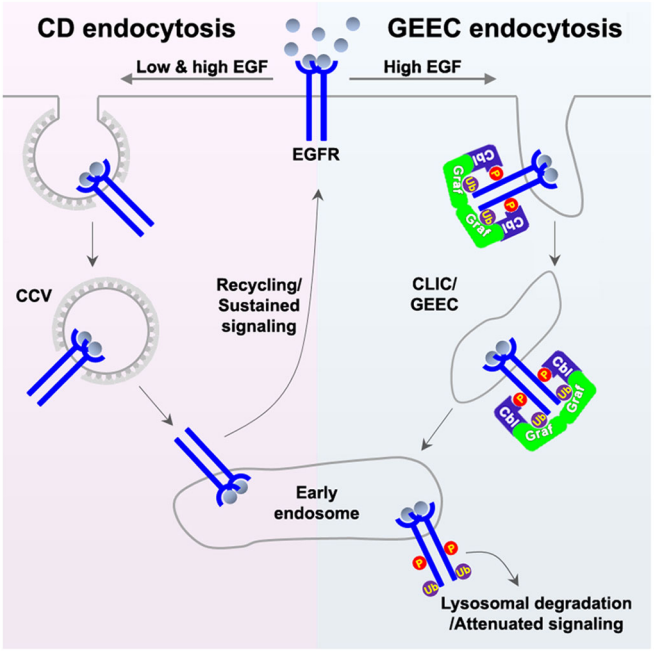

Fig. 8. Model for differential EGFR regulation by CD and GEEC endocytosis. At low doses of EGF, EGFR is largely internalized through CD endocytosis, which primarily results in receptor recycling and sustained signaling (Sigismund et al., 2008, 2005). At high doses of EGF, a substantial fraction of EGFR is internalized through Graf-dependent GEEC endocytosis, which primarily targets internalized receptors to degradation, causing signal attenuation. Under the latter condition, Cbl is recruited to and ubiquitylates phosphorylated EGFRs. This post-translational modification enhances physical interactions between EGFR and Graf to promote GEEC endocytosis of the receptor. CCV, clathrin-coated vesicle.

Development (2017) 144, 4159-4172 doi:10.1242/dev.153288

domain enhances its ability to interact with Graf *in vitro*. Given this Graf/Ub-dependent sorting mechanism, it will be interesting in the future to determine whether other receptor tyrosine kinases (RTKs) subjected to D-Cbl-mediated ubiquitylation are internalized through Graf-dependent GEEC endocytosis, resulting in their degradation.

At present, the mechanism by which loss of GRAF1 causes AML or MDS remains unknown. Our *Drosophila* studies reveal that EGFR overexpression is the principal force driving the selective overproliferation of a myeloid-like lineage (plasmatocytes) in *Graf*-null mutant larvae, suggesting a potential link between EGFR dysregulation and myeloid malignancies. Consistent with this possibility, one recent clinical study reported elevated expression of EGFR protein in ∼33% of primary AML samples and associated this elevated expression with poor clinical outcomes (Sun et al., 2012). In addition, another clinical study reported EGFR mutations in primary malignant cells from individuals with MDS (Bejar et al., 2011). Furthermore, administration of the EGFR inhibitor erlotinib can cause complete remission of AML in individuals with concomitant non-small-cell lung cancer, although its off-target effects on Jak2 were invoked to explain this anti-neoplastic activity (Chan and Pilichowska, 2007; Pitini et al., 2008). These clinical data, combined with our current findings, suggest that EGFR dysregulation may contribute to the development and progression of a subset of myeloid malignancies. Future experiments will further address this important issue.

MATERIALS AND METHODS

Fly stocks

Flies were maintained at 25°C. The fly strains used and the generation of transgenic lines are detailed in the supplementary Materials and Methods.

Molecular biology

A full-length cDNA for *Graf* was amplified by reverse transcription (RT)-PCR of total RNA extracted from *Drosophila* S2R+ cells and then cloned into the pGEM-T Easy vector (Promega). For transgenic rescue experiments, a full-length cDNA for *Graf* was subcloned into pcDNA3.1-HA, a derivative of the pcDNA3.1(+) vector (Invitrogen), and then subcloned again with the C-terminal HA-tag sequence into the pUAST vector (Brand and Perrimon, 1993) to produce *UAS-Graf-HA*. For expression of Graf-GFP in S2R+ cells, the *Graf* cDNA insert was subcloned into the pAc-EGFP vector (Invitrogen). For expression of GST-Graf and His_6-Graf in *E. coli*, the full-length *Graf* cDNA was subcloned into the pGEX6P1 vector (GE Healthcare) or the pRSET A vector (Invitrogen), respectively.

For expression of additional genes in S2R+ cells or *E. coli*, their cDNAs were subcloned into the pUAST, pAc5.1, or pGEX6P1 vector. See the supplementary Materials and Methods for the construction of *UAS-Myc-arf1*, *UAS-Myc-Rab5*, *UAS-Myc-Cdc42-Q61L*, *UAS-Flag-Egfr*, *UAS-Flag-Egfr-Y1271F*, *pAc-sSpi-GFP*, *pAc-sSpi-HA*, *pAc-HA-Ub* and *pGEX6P1-Egfr-IC-Ub*. The *UAS-GFP-GPI* construct was obtained from the *Drosophila* Genomics Resource Center.

To characterize the *Graf* excision lines, genomic DNA was isolated from homozygous animals and used as a template for PCR using the following primers: 5′-TACAGGATCATACCTGTGACTAC-3′ and 5′-GCTTGACCATCGATTATTTCTGG-3′. PCR products were subcloned and subjected to DNA sequencing to identify the precise breakpoints of each *Graf* deletion. RT-PCR was performed to assess the effect of the $Graf^1$ mutation on the expression of *Graf*, as detailed in the supplementary Materials and Methods.

For RNAi experiments in S2R+ cells, *Graf*, *chc*, *arf1* and *D-cbl* dsRNAs were generated by *in vitro* transcription of their cognate DNA templates containing T7 promoters at both ends, as previously described (Lee et al., 2007). See the supplementary Materials and Methods for the generation of DNA templates for *in vitro* transcription.

Cell transfection and production of Spi-conditioned medium

Drosophila S2R+ cells were maintained at 25°C in Schneider's medium (Invitrogen) supplemented with 10% heat-inactivated (30 min, 55°C) fetal bovine serum (FBS) and antibiotics. S2R+ cells were transfected using Cellfectin (Invitrogen), according to the manufacturer's instructions. Typically, 10^6 cells were transfected in serum-free medium with 2 µg of plasmid DNA or 5 µg of double-stranded RNA (dsRNA). Expression of all UAS plasmids was driven by co-transfection of RK241, an *actin 5C-GAL4* plasmid.

For production of Spi-conditioned medium, transfection of S2R+ cells with *pAc-sSpi-HA* or *pAc-sSpi-GFP* was performed in serum-free medium for 4 h. Transfected cells were incubated for 48 h in serum-containing medium and then for 24 h in fresh serum-free medium. Levels of secreted sSpi-GFP and sSpi-HA in the conditioned medium were measured by ELISA (Cell Biolabs) and western blot analysis using a multiple-epitope tag (GenScript). To treat primary larval hemocytes and S2R+ cells, the conditioned medium was diluted with serum-free Schneider's medium to 4 ng/ml or 30 ng/ml sSpi-GFP (to obtain a final concentration of about 1.3 ng/ml or 10 ng/ml sSpi) or 10 ng/ml sSpi-HA.

Antibodies

Antibodies used for immunostaining and western blotting are described in the supplementary Materials and Methods.

Western blotting and binding experiments

Western blotting, co-immunoprecipitation and GST pull-down assays were performed as described previously (Nahm et al., 2010), with some modifications. For details, see the supplementary Materials and Methods.

Immunostaining

Fixed and permeabilized embryos, primary hemocytes, and S2R+ cells were stained with the indicated antibodies and imaged by confocal microscopy. For further details, see the supplementary Materials and Methods.

Fluorescence-based internalization and trafficking studies

For sSpi-GFP internalization assays, primary hemocytes from early third instar larvae were incubated in conditioned medium containing 4 or 30 ng/ml of sSpi-GFP for 30 min at 4°C to allow the ligand to bind to surface EGFRs. In some experiments, 20 µM dynasore (Sigma) was also pretreated to inhibit dynamin. After washing with ice-cold PBS, hemocytes were incubated in serum-free Schneider's medium for 2 min at 25°C to allow internalization of sSpi-GFP. Hemocytes were immediately fixed on ice for 10 min with ice-cold 4% formaldehyde in PBS and permeabilized with PBST-0.2 for 10 min and then stained with an anti-GFP antibody and an appropriate fluorescent-conjugated secondary antibody. For each cell, a *z* stack of images was taken with a LSM 700 laser-scanning confocal microscope (Carl Zeiss) using a Plan Apo 63×1.4 NA oil objective. To quantify the amount of internalized sSpi-GFP, total fluorescence per cell was determined by integrating intracellular fluorescence on all planes of the *z* stack after correcting for background fluorescence.

For sSpi-GFP trafficking studies, primary hemocytes pretreated with 4 or 30 ng/ml of sSpi-GFP for 30 min at 4°C were incubated at 25°C for 2 min or 25 min. Hemocytes were immediately processed for staining with anti-GFP and anti-Graf or anti-Chc antibodies (2 min internalization) or further incubated with 1 µM Lysotracker (Molecular Probes) for 5 min (25 min internalization), prior to staining with an anti-GFP antibody. Fluorescence imaging was done with a LSM 700 laser-scanning confocal microscope (Carl Zeiss) using a Plan Apo 63×1.4 NA oil objective. For quantitative analysis of anti-GFP and Graf/Chc/Lysotracker colocalization, a *z* stack of two-dimensional images (0.35 µm thick) of cells was obtained through FITC (sSpi-GFP) and Cy3 (Graf, Chc, or Lysotracker) filter channels and deconvoluted using the AutoQuant software (Media Cybernetics). Quantitative analysis was performed on deconvoluted *z* stack images using the JACoP plug-in for ImageJ to determine Manders' coefficient M_1, which represents the ratio of the summed intensities of pixels from the green image for which the intensity on the red channel is above 0 to the total intensity in the green channel. Details on the analysis of endocytic probe

Development (2017) 144, 4159-4172 doi:10.1242/dev.153288

internalization with primary hemocytes and EGFR trafficking studies in S2R+ cells can be found in the supplementary Materials and Methods.

EGFR degradation assay

S2R+ cells overexpressing Flag-EGFR were stimulated with 30 ng/ml sSpi-GFP for the indicated time and subjected to western blot analysis. For further details, see the supplementary Materials and Methods.

Hemocyte counting and statistical analysis

For hemocyte counting, late-wandering third instar larvae were staged using food containing 0.5% green household food dye as described previously (Zettervall et al., 2004). For further details, see the supplementary Materials and Methods.

The collected values were analyzed for normality with the D'Agostino-Pearson omnibus test and used for significance testing. To determine statistical significance, we performed the Student's *t*-test or one-way ANOVA followed by post hoc pairwise comparisons of means using Tukey-Kramer test.

Acknowledgements

We are grateful to the Bloomington, VRDC and Kyoto *Drosophila* stock centers, to the DSHB hybridoma bank, and to the following individuals for stocks and reagents: I. Ando, K. Bruckner, J. Jiang, M. Haenlin, E. Hafen, L.-M. Pai, and B.-Z. Shilo.

Competing interests

The authors declare no competing or financial interests.

Author contributions

Conceptualization: S.K., S.C., E.Y.C., J.S., C.L., S.L.; Methodology: S.K., M.N., N.K., Y.K., J.K., J.S.; Investigation: S.L.; Writing - original draft: S.K., M.N., S.L.; Writing - review & editing: S.C., E.Y.C.; Supervision: C.L., S.L.; Funding acquisition: S.L.

Funding

This work was supported by grants from the National Research Foundation of Korea (2010-0027941 and 2017M3C7A1025368) and the BK+ program of the National Research Foundation of Korea.

Supplementary information

Supplementary information available online at
http://dev.biologists.org/lookup/doi/10.1242/dev.153288.supplemental

References

Asha, H., Nagy, I., Kovacs, G., Stetson, D., Ando, I. and Dearolf, C. R. (2003). Analysis of Ras-induced overproliferation in Drosophila hemocytes. *Genetics* **163**, 203-215.

Avraham, R. and Yarden, Y. (2011). Feedback regulation of EGFR signalling: decision making by early and delayed loops. *Nat. Rev. Mol. Cell Biol.* **12**, 104-117.

Bejar, R., Stevenson, K., Abdel-Wahab, O., Galili, N., Nilsson, B., Garcia-Manero, G., Kantarjian, H., Raza, A., Levine, R. L., Neuberg, D. et al. (2011). Clinical effect of point mutations in myelodysplastic syndromes. *N. Engl. J. Med.* **364**, 2496-2506.

Bojesen, S. E., Ammerpohl, O., Weinhäusl, A., Haas, O. A., Mettal, H., Bohle, R. M., Borkhardt, A. and Fuchs, U. (2006). Characterisation of the GRAF gene promoter and its methylation in patients with acute myeloid leukaemia and myelodysplastic syndrome. *Br. J. Cancer* **94**, 323-332.

Borkhardt, A., Bojesen, S., Haas, O. A., Fuchs, U., Bartelheimer, D., Loncarevic, I. F., Bohle, R. M., Harbott, J., Repp, R., Jaeger, U. et al. (2000). The human GRAF gene is fused to MLL in a unique t(5;11)(q31;q23) and both alleles are disrupted in three cases of myelodysplastic syndrome/acute myeloid leukemia with a deletion 5q. *Proc. Natl. Acad. Sci. USA* **97**, 9168-9173.

Brand, A. H. and Perrimon, N. (1993). Targeted gene expression as a means of altering cell fates and generating dominant phenotypes. *Development* **118**, 401-415.

Chan, G. and Pilichowska, M. (2007). Complete remission in a patient with acute myelogenous leukemia treated with erlotinib for non small-cell lung cancer. *Blood* **110**, 1079-1080.

Crozatier, M. and Vincent, A. (2011). Drosophila: a model for studying genetic and molecular aspects of haematopoiesis and associated leukaemias. *Dis. Model Mech.* **4**, 439-445.

Evans, C. J., Hartenstein, V. and Banerjee, U. (2003). Thicker than blood: conserved mechanisms in Drosophila and vertebrate hematopoiesis. *Dev. Cell* **5**, 673-690.

Francis, M. K., Holst, M. R., Vidal-Quadras, M., Henriksson, S., Santarella-Mellwig, R., Sandblad, L. and Lundmark, R. (2015). Endocytic membrane turnover at the leading edge is driven by a transient interaction between Cdc42 and GRAF1. *J. Cell Sci.* **128**, 4183-4195.

Guha, A., Sriram, V., Krishnan, K. S. and Mayor, S. (2003). Shibire mutations reveal distinct dynamin-independent and -dependent endocytic pathways in primary cultures of Drosophila hemocytes. *J. Cell Sci.* **116**, 3373-3386.

Gupta, G. D., Swetha, M. G., Kumari, S., Lakshminarayan, R., Dey, G. and Mayor, S. (2009). Analysis of endocytic pathways in Drosophila cells reveals a conserved role for GBF1 in internalization via GEECs. *PLoS ONE* **4**, e6768.

Holz, A., Bossinger, B., Strasser, T., Janning, W. and Klapper, R. (2003). The two origins of hemocytes in Drosophila. *Development* **130**, 4955-4962.

Kalia, M., Kumari, S., Chadda, R., Hill, M. M., Parton, R. G. and Mayor, S. (2006). Arf6-independent GPI-anchored protein-enriched early endosomal compartments fuse with sorting endosomes via a Rab5/phosphatidylinositol-3'-kinase-dependent machinery. *Mol. Biol. Cell* **17**, 3689-3704.

Kirkham, M., Fujita, A., Chadda, R., Nixon, S. J., Kurzchalia, T. V., Sharma, D. K., Pagano, R. E., Hancock, J. F., Mayor, S. and Parton, R. G. (2005). Ultrastructural identification of uncoated caveolin-independent early endocytic vehicles. *J. Cell Biol.* **168**, 465-476.

Kumari, S. and Mayor, S. (2008). ARF1 is directly involved in dynamin-independent endocytosis. *Nat. Cell Biol.* **10**, 30-41.

Lanot, R., Zachary, D., Holder, F. and Meister, M. (2001). Postembryonic hematopoiesis in Drosophila. *Dev. Biol.* **230**, 243-257.

Lebestky, T., Chang, T., Hartenstein, V. and Banerjee, U. (2000). Specification of Drosophila hematopoietic lineage by conserved transcription factors. *Science* **288**, 146-149.

Lee, S., Nahm, M., Lee, M., Kwon, M., Kim, E., Zadeh, A. D., Cao, H., Kim, H.-J., Lee, Z. H., Oh, S. B. et al. (2007). The F-actin-microtubule crosslinker Shot is a platform for Krasavietz-mediated translational regulation of midline axon repulsion. *Development* **134**, 1767-1777.

Levkowitz, G., Waterman, H., Zamir, E., Kam, Z., Oved, S., Langdon, W. Y., Beguinot, L., Geiger, B. and Yarden, Y. (1998). c-Cbl/Sli-1 regulates endocytic sorting and ubiquitination of the epidermal growth factor receptor. *Genes Dev.* **12**, 3663-3674.

Levkowitz, G., Waterman, H., Ettenberg, S. A., Katz, M., Tsygankov, A. Y., Alroy, I., Lavi, S., Iwai, K., Reiss, Y., Ciechanover, A. et al. (1999). Ubiquitin ligase activity and tyrosine phosphorylation underlie suppression of growth factor signaling by c-Cbl/Sli-1. *Mol. Cell* **4**, 1029-1040.

Lundmark, R., Doherty, G. J., Howes, M. T., Cortese, K., Vallis, Y., Parton, R. G. and McMahon, H. T. (2008). The GTPase-activating protein GRAF1 regulates the CLIC/GEEC endocytic pathway. *Curr. Biol.* **18**, 1802-1808.

Makhijani, K., Alexander, B., Tanaka, T., Rulifson, E. and Bruckner, K. (2011). The peripheral nervous system supports blood cell homing and survival in the Drosophila larva. *Development* **138**, 5379-5391.

Nahm, M., Long, A. A., Paik, S. K., Kim, S., Bae, Y. C., Broadie, K. and Lee, S. (2010). The Cdc42-selective GAP rich regulates postsynaptic development and retrograde BMP transsynaptic signaling. *J. Cell Biol.* **191**, 661-675.

Panagopoulos, I., Kitagawa, A., Isaksson, M., Mörse, H., Mitelman, F. and Johansson, B. (2004). MLL/GRAF fusion in an infant acute monocytic leukemia (AML M5b) with a cytogenetically cryptic ins(5;11)(q31;q23q23). *Genes Chromosomes Cancer* **41**, 400-404.

Patel, R. and Leung, H. Y. (2012). Targeting the EGFR-family for therapy: biological challenges and clinical perspective. *Curr. Pharm. Des.* **18**, 2672-2679.

Pitini, V., Arrigo, C. and Altavilla, G. (2008). Erlotinib in a patient with acute myelogenous leukemia and concomitant non-small-cell lung cancer. *J. Clin. Oncol.* **26**, 3645-3646.

Qian, Z., Qian, J., Lin, J., Yao, D.-M., Chen, Q., Ji, R.-B., Li, Y., Xiao, G. F. and Li, J.-Y. (2010). GTPase regulator associated with the focal adhesion kinase (GRAF) transcript was down-regulated in patients with myeloid malignancies. *J. Exp. Clin. Cancer Res.* **29**, 111.

Qian, J., Qian, Z., Lin, J., Yao, D.-M., Chen, Q., Li, Y., Ji, R.-B., Yang, J., Xiao, G.-F. and Wang, Y.-L. (2011). Abnormal methylation of GRAF promoter Chinese patients with acute myeloid leukemia. *Leuk. Res.* **35**, 783-786.

Rutledge, B. J., Zhang, K., Bier, E., Jan, Y. N. and Perrimon, N. (1992). The Drosophila spitz gene encodes a putative EGF-like growth factor involved in dorsal-ventral axis formation and neurogenesis. *Genes Dev.* **6**, 1503-1517.

Sabharanjak, S., Sharma, P., Parton, R. G. and Mayor, S. (2002). GPI-anchored proteins are delivered to recycling endosomes via a distinct cdc42-regulated, clathrin-independent pinocytic pathway. *Dev. Cell* **2**, 411-423.

Sakaue-Sawano, A., Kurokawa, H., Morimura, T., Hanyu, A., Hama, H., Osawa, H., Kashiwagi, S., Fukami, K., Miyata, T., Miyoshi, H. et al. (2008). Visualizing spatiotemporal dynamics of multicellular cell-cycle progression. *Cell* **132**, 487-498.

Shilo, B. Z. (2003). Signaling by the Drosophila epidermal growth factor receptor pathway during development. *Exp. Cell Res.* **284**, 140-149.

Sigismund, S., Woelk, T., Puri, C., Maspero, E., Tacchetti, C., Transidico, P., Di Fiore, P. P. and Polo, S. (2005). Clathrin-independent endocytosis of ubiquitinated cargos. *Proc. Natl. Acad. Sci. USA* **102**, 2760-2765.

Sigismund, S., Argenzio, E., Tosoni, D., Cavallaro, E., Polo, S. and Di Fiore, P. P. (2008). Clathrin-mediated internalization is essential for sustained EGFR signaling but dispensable for degradation. *Dev. Cell* **15**, 209-219.

Development (2017) 144, 4159-4172 doi:10.1242/dev.153288

Sigismund, S., Algisi, V., Nappo, G., Conte, A., Pascolutti, R., Cuomo, A., Bonaldi, T., Argenzio, E., Verhoef, L. G. G. C., Maspero, E. et al. (2013). Threshold-controlled ubiquitination of the EGFR directs receptor fate. *EMBO J.* **32**, 2140-2157.

Sinenko, S. A., Shim, J. and Banerjee, U. (2011). Oxidative stress in the haematopoietic niche regulates the cellular immune response in Drosophila. *EMBO Rep.* **13**, 83-89.

Sorkin, A. and Goh, L. K. (2009). Endocytosis and intracellular trafficking of ErbBs. *Exp. Cell Res.* **315**, 683-696.

Sun, J.-Z., Lu, Y., Xu, Y., Liu, F., Li, F.-Q., Wang, Q.-L., Wu, C.-T., Hu, X.-W. and Duan, H.-F. (2012). Epidermal growth factor receptor expression in acute myelogenous leukaemia is associated with clinical prognosis. *Hematol. Oncol.* **30**, 89-97.

Tepass, U., Fessler, L. I., Aziz, A. and Hartenstein, V. (1994). Embryonic origin of hemocytes and their relationship to cell death in Drosophila. *Development* **120**, 1829-1837.

Wilda, M., Perez, A. V., Bruch, J., Woessmann, W., Metzler, M., Fuchs, U. and Borkhardt, A. (2005). Use of MLL/GRAF fusion mRNA for measurement of minimal residual disease during chemotherapy in an infant with acute monoblastic leukemia (AML-M5). *Genes Chromosomes Cancer* **43**, 424-426.

Zettervall, C.-J., Anderl, I., Williams, M. J., Palmer, R., Kurucz, E., Ando, I. and Hultmark, D. (2004). A directed screen for genes involved in Drosophila blood cell activation. *Proc. Natl. Acad. Sci. USA* **101**, 14192-14197.